Electronic Supplementary Material (ESI) for RSC Advances.

Supporting Information

Nitrogen-doped carbon derived from horse manure biomass as a catalyst for the oxygen reduction reaction†

Gasidit Panomsuwan[a,b,c*], Chadapat Hussakan[a,b], Napat Kaewtrakulchai[d], Ratchatee Techapiesancharoenkij[a,b], Ai Serizawa[e], Takahiro Ishizaki[e], and Apiluck Eiad-ua[f,*]

[a] Department of Materials Engineering, Faculty of Engineering, Kasetsart University, Bangkok 10900, Thailand

[b] International Collaborative Education Program for Materials Technology, Education, and Research (ICE-Matter), ASEAN University Network/Southeast Asia Engineering Education Development Network (AUN/SEED-Net), Kasetsart University, Bangkok 10900, Thailand

[c] Special Research Unit for Biomass Conversion Technology for Energy and Environmental Materials, Kasetsart University, Bangkok 10900, Thailand

[d] Kasetsart Agricultural and Agro-Industrial Product Improvement Institute, Kasetsart University, Bangkok 10900, Thailand

[e] Department of Materials Science and Engineering, Faculty of Engineering, Shibaura Institute of Technology, Tokyo 135-8548, Japan

[f] College of Materials Innovation and Technology, King Mongkut's Institute of Technology Ladkrabang, Bangkok 10520, Thailand

[*]Corresponding authors: gasidit.p@ku.ac.th (G. Panomsuwan); apiluck.ei@kmitl.ac.th (A. Eiad-ua)

Table S1. Production yields of hydrochars and HMNCs derived from horse manure at different ammonia concentrations.

Sample	Hydrochar yield (%)	HMNC yield (%)
HMNC-0	74.12	31.24
HMNC-0.5	71.72	27.31
HMNC-1.0	68.26	26.57
HMNC-1.5	65.73	23.92

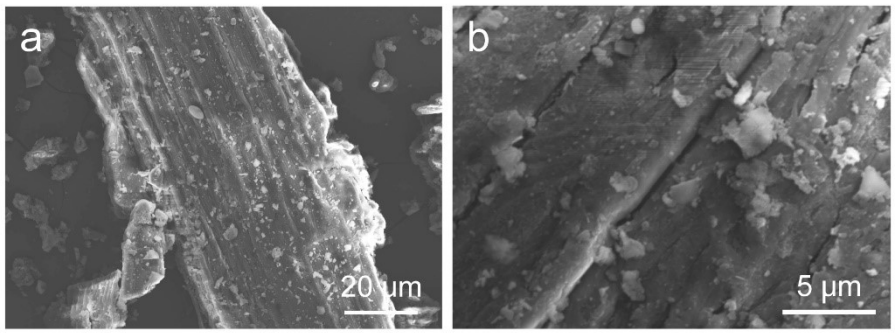

Fig. S1. SEM image of horse manure.

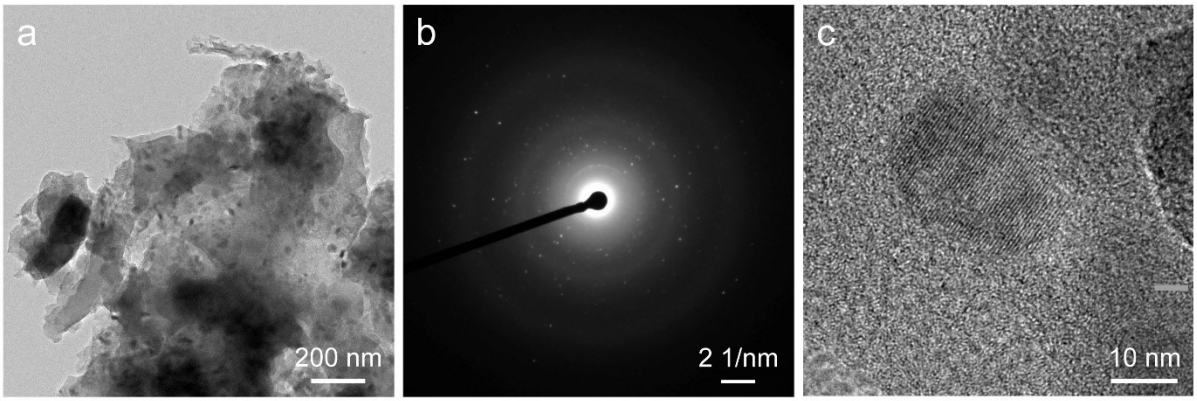

Fig. S2. TEM images and SAED pattern of HMNC-1.0.

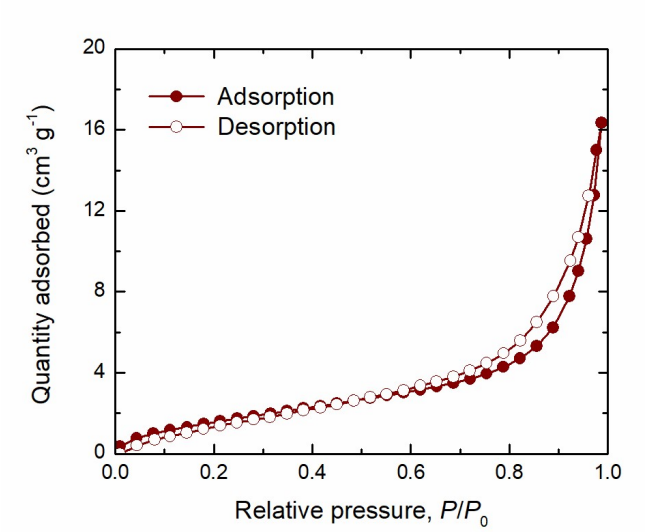

Fig. S3. N_2 adsorption-desorption isotherm of horse manure.

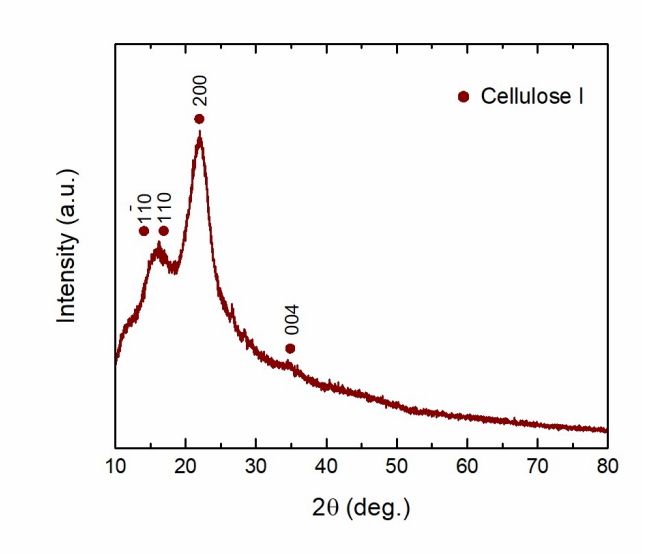

Fig. S4. XRD pattern of horse manure corresponding to the crystalline cellulose I structure.

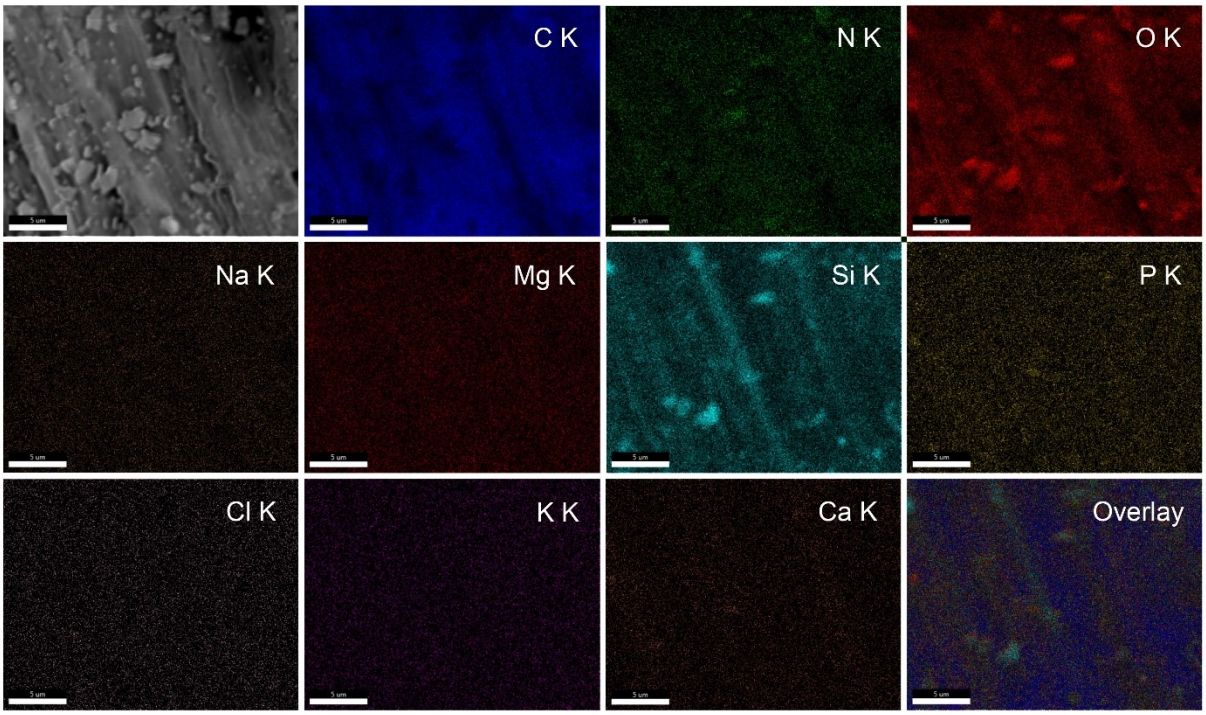

Fig. S5. SEM-EDS mapping analysis of horse manure.

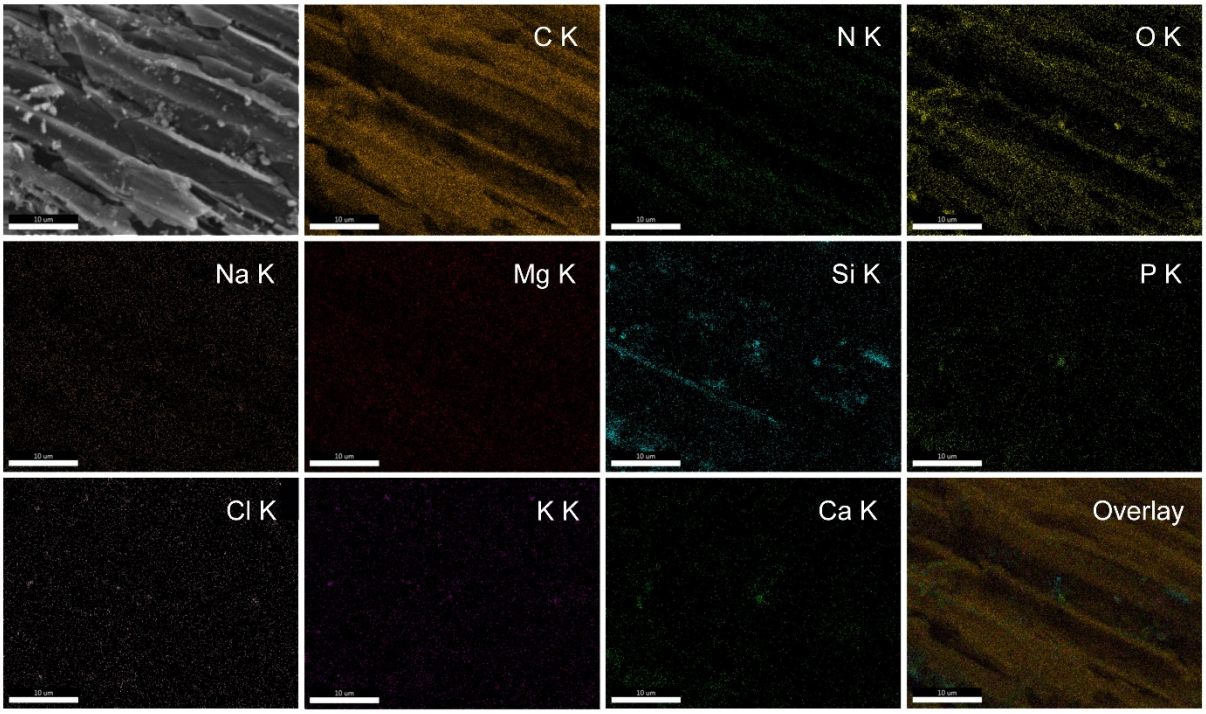

Fig. S6. SEM-EDS mapping analysis of HMNC-1.0.

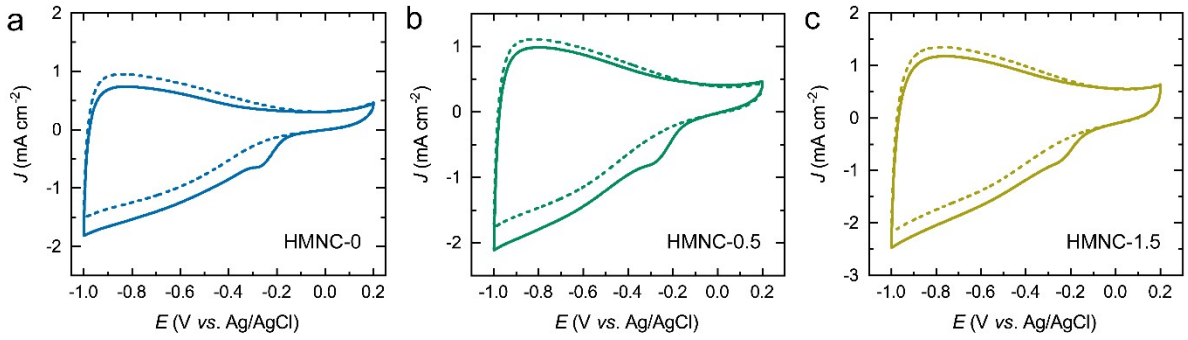

Fig. S7. CV curves measured in 0.1 M KOH solution with the saturation of N_2 (dashed line) and O_2 (solid line) at a scan rate of 50 mV s^{-1}: (a) HMNC-0, (b) HMNC-0.5, and (c) HMNC-1.5.

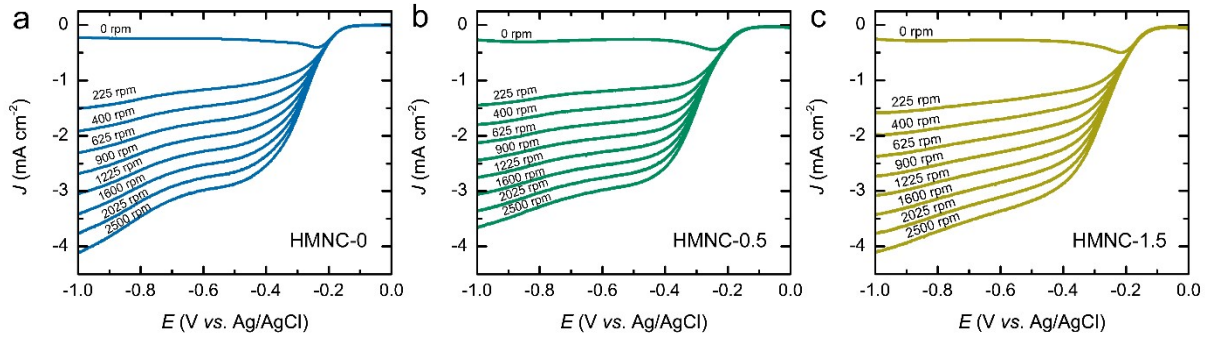

Fig. S8. LSV curves measured at various rotation speeds from 225 to 2500 rpm in O_2-saturated 0.1 M KOH solution at a scan rate of 10 mV s^{-1}: (a) HMNC-0, (b) HMNC-0.5, and (c) HMNC-1.5. Note: The current density was subtracted from the capacitive current measured in the N_2-saturated electrolyte.

Table S2. Comparison ORR results of the biomass-derived nitrogen-doped carbon materials in 0.1 M KOH. The ORR onset potential (E_{onset}) and half-wave potential ($E_{1/2}$) in O_2-saturated 0.1 M KOH are given with respect to Ag/AgCl.

Catalysts	Biomass	Surface area ($m^2\ g^{-1}$)	Pore volume ($cm^3\ g^{-1}$)	Nitrogen content (atom%)	E_{onset} (V)	Electron transfer number (n)	Catalyst loading ($mg\ cm^{-2}$)	Reference
CD	Cow dung	128.5	0.091	-	–0.12	-	0.203	S1
CS	Chitin	100	0.06	3.69	–0.17	3.63 @–0.7 V	0.202	S2
NCA-K-900	Chicken feather rachis	183.2	0.238	2.3	–0.02	3.5 @–0.7 V 2.5 @–0.5 V	-	S3
CCB	Chicken bone	69	-	-	–0.19	-	-	S4
CCB_1	Chicken bone	294	-	-	–0.12	-	-	S4
CN_x-1000	Poutry feather	-	-	8.2	–0.195	-	0.353	S5
CN_x-950	Chicken feather rachis	4.77	-	2.3	–0.20	-	1.777	S6
CNA_x-900	Chicken feather rachis	301.2	-	4.3	–0.02	-	1.777	S6
N-GLC	Bagasse	530			0.07	~4 @–0.4 V	0.750	S7
CNPs-800	*Allium sativum*	234.1	0.14	-	–0.08	3.8 @–0.5 V	-	S8
N-QD	Unripe peach	-	-	8.77	–0.05	1.82 @–0.7 V	1.76	S9
N-HPC	*Allium cepa*	1607	-	-	–0.10	3.3 @–0.4 V	0.141	S10
BCM	Pomelo peel	62.8	0.03	0.51	–0.23	3.2 @–0.4 V	-	S11
a-BCM	Pomelo peel	314.3	0.22	2.41	–0.08	3.6 @–0.4 V	-	S11
HMNC-1.0	Horse manure	55.2	0.055	1.32	–0.15	2.70 @–0.4V	0.398	This work

References

[S1] Z. Zhang, H. Li, Y. Yang, J. Key, S. Ji, Y. Ma, H. Wang and R. Wang, *RSC Adv*. 2015, **5**, 27112–27119.

[S2] H. Yuan, L. Deng, X. Cai, S. Zhou, Y. Chen and Y. Yuan, *RSC Adv.* 2015, **5**, 56121–56129.

[S3] A. Tyagi, A. Yadav, P. Sinha, S. Singh, P. Paik and K. K. Kar, *Appl. Surf. Sci.* 2019, **495**, 143603.

[S4] H. Song, H. Li, H. Wang, J. Key, S. Ji, X. Mao, R. Wang, *Electrochim. Acta* 2014, **147**, 520–526.

[S5] R. Sharma and K. K. Kar, *Electrochim. Acta* 2016, **191**, 876–886.

[S6] A. Tyagi, S. Banarjee, S. Singh and K. K. Kar, *Int. J. Hydrogen Energy* 2020, **45**, 16930–16943.

[S7] D. Bosubabu, V. Parthiban, A. K. Sahu and K. Ramesha, *Bull. Mater. Sci.* 2021, **44**, 135.

[S8] P. Kanagavalli, G. R. Pandey, V. S. Bhat, M. Veerapandian, G. Hedge, *J. Nanostruct. Chem.* 2021, **11**, 343–352.

[S9] R. A. Thomas, N. Jebakumar, I. Edison and Y. R. Lee, *J. Colloid. Interf. Sci.* 2016, **482**, 8–18.

[S10] J. Zhang, J. He, H. Zheng, R. Li and X. Gou, *J. Mater. Sci.* 2020, **55**, 7464–7476.

[S11] Y. Zhang, L. Deng, H. Hu, Y. Qiao, H. Yuan, D. Chen, M. Chang and H. Wei, *Sustain. Energy Fuels* 2020, **4**, 1642–1653.